High-frequency electromagnon in $GdMnO_3$

A.M. Shuvaev[1], F. Mayr[2], A. Loidl[2], A.A. Mukhin[3], and A. Pimenov[1,a]

[1] Institute of Solid State Physics, Vienna University of Technology, 1040 Vienna, Austria
[2] Experimentalphysik V, EKM, Universität Augsburg, 86135 Augsburg, Germany
[3] General Physics Institute, Russian Academy of Sciences, 119991 Moscow, Russia

Abstract. Results of far-infrared transmittance are reported for $GdMnO_3$, a multiferroic perovskite manganite. The spectra allow to obtain position and intensity of the high-frequency electromagnon ($\sim$75 cm^{-1}) in this material. We present a comparative analysis of the high- and low-frequency electromagnons across the phase diagram of $GdMnO_3$. The traces of the electromagnon excitation can be detected even deeply in the paramagnetic state, which is attributed to magnetic fluctuations.

1 Introduction

Multiferroics are materials which simultaneously reveal magnetic and polar electric order [1–3]. The enormous recent theoretical and experimental interest in these systems results from new exciting physics and potential applications, especially in memory devices. Multiferroics are often characterized by a strong coupling between magnetism and electricity leading to such effects like switching of the electric polarization in external magnetic fields [4] or manipulation of magnetic properties by electric fields [5].

The dynamic properties of multiferroics are quite rich as well. In addition to classical modes of the ordered magnetic structure, multiferroics show the existence of new excitations of magnetoelectric nature [6–8]. These excitations have been called electromagnons and represent magnetic modes which can be excited by the electric component of the electromagnetic radiation. The dynamics of $TbMnO_3$ is very instructive in this context, because optical experiments in this material [9–11] can be combined with the results by inelastic neutron scattering [12,13]. Closely related systems, like $GdMnO_3$ or $DyMnO_3$ in many aspects reveal a similar dynamics. The electromagnon excitations in these materials seem to consist of two modes [7,8]. A strong high-frequency electromagnon is observed in the frequency range 60–90 cm^{-1}. The frequency of this mode corresponds to a zone edge magnon as experimentally proven by inelastic neutron scattering experiments [13]. The spectral weight and excitation conditions for this mode can well be explained [11,14] by the Heisenberg exchange mechanism combined with a modulation of the magnetic structure. In addition, another electromagnon has been identified in the frequency range close to 20 cm^{-1}. The origin of this mode, which is often split into two modes [6], is not fully understood. The characteristic position of the low-frequency electromagnon seems to correspond [15,16] to a magnon at the center of the magnetic Brillouin zone [13]. In this scenario, the zone center magnons are electrically active modes of the cycloidal magnetic structure and receive electric dipolar weight due to an inverse Dzyaloshinskii-Moriya mechanism [6,17]. As this mechanism cannot explain the intensity and the excitation conditions of the modes, the model based on the Heisenberg exchange and including the magnetic anisotropy has been suggested [18,19]. A comparison of the model predictions with the experimental parameters may help to resolve the problems with the origin of electromagnons. Therefore, systematic investigations of dynamical properties of different multiferroics remain an actual task.

$GdMnO_3$ reveals an incommensurate (IC) antiferromagnetic (AFM) phase below $T_N = 42$ K. This phase probably is characterized by a sinusoidally modulated spin structure of the manganese spins, with the Gd spins still remaining paramagnetic [20–22]. In low external magnetic fields fields ($B < 0.1$ T) and under zero-field cooling conditions the IC structure remains the stable phase down to $T = 8$ K and is followed by a complex canted ferrimagnetic structure of Gd and Mn spins. In finite magnetic fields along the c-axis the IC-AFM phase is transformed to a canted antiferromagnetic (CA-AFM) state. Between 8 K and 17 K this spin arrangement strongly competes with the IC-AFM phase and depending on the magnetic history the canted antiferromagnet can be stabilized even in zero external magnetic fields. We note that, strictly speaking, $GdMnO_3$ cannot be called multiferroic because no ferroelectric polarization has been observed in this material at least in zero external magnetic field [20,22]. We will return to this point in the Results and Discussion section.

In this work we have carried out infrared transmittance experiments in multiferroic $GdMnO_3$. The combination of these data with the results by terahertz experiments [9]

[a] e-mail: andrei.pimenov@ifp.tuwien.ac.at

allowed to carry out a comparative analysis of low- and high-frequency electromagnons in this material.

2 Experimental details

Single crystals of $GdMnO_3$ have been prepared using the floating-zone method with radiation heating [23]. The samples have been characterized using X-ray, magnetic and dielectric measurement [21,22]. The basic properties of our samples agree well with the results obtained by other groups [20,24]. Transmittance spectra in the infrared frequency range have been obtained using a Bruker IFS-113 Fourier-transform spectrometer. For this purpose the *ab*-oriented cut of the crystal was polished down to the thickness of 220 μm. Reflectance spectra in the infrared frequency range have been measured on a thick sample from the same batch and were published elsewhere [25]. At this point we note that in spite of the relatively large intensity of the electromagnons, these modes can hardly be detected in reflectance spectra. Although the reflectance derived spectra [25] do show some characteristic feature around 75 cm^{-1}, without transmittance experiments the high-frequency electromagnon could not be observed unambiguously. In present work, in order to obtain the full picture of the electromagnons, the results by infrared transmittance are combined with terahertz spectra, as obtained previously using the BWO-type technique [9].

3 Results and discussion

Figure 1 shows transmittance spectra of a thin $GdMnO_3$ sample in the far infrared frequency range. The strongest absorption is observed close to 120 cm^{-1}, which corresponds to the lowest phonon in $GdMnO_3$. Close to this phonon the transmittance is below the sensitivity level of the spectrometer. Most importantly, a broad minimum in transmittance can be seen around 75 cm^{-1} corresponding to the high-frequency electromagnon. Figure 1 documents that with increasing temperature the intensity of the electromagnon gradually decreases, which corresponds to the increase of the transmission level. Even at $T = 70$ K, i.e. deep in the paramagnetic state, a local minimum in transmittance close to 75 cm^{-1} can be seen indicating nonzero electromagnon intensity at this temperature. The presented data are sufficient to fill in the frequency gap between previous experiments [9,25] in $GdMnO_3$, which gave reliable spectra above 100 cm^{-1} and below 40 cm^{-1}.

The measured transmittance spectra have been transformed into the dielectric permittivity by inverting the Fresnel optical equations for transmittance and reflectivity neglecting the interferences within the sample. These interferences are seen as a Fabry-Pérot type modulation of the transmittance spectra in Figure 1 and they are especially clear between 20 cm^{-1} and 60 cm^{-1} and at room temperature. An attempt to take into account the interferences did not improve the quality of the solution probably due to imperfections of the sample surface. The results of the data processing are given in Figure 2 which

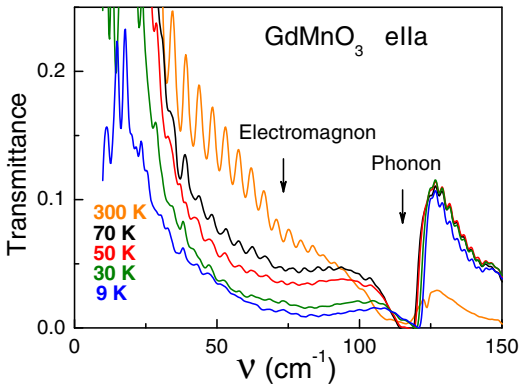

Fig. 1. (Color online) Transmittance spectra of a thin $GdMnO_3$ sample in the far-infrared frequency range and at different temperatures as indicated. Arrows show the position of the high-frequency electromagnon and of the lowest infrared phonon. The low-frequency electromagnon (around 23 cm^{-1}) is not seen in this presentation.

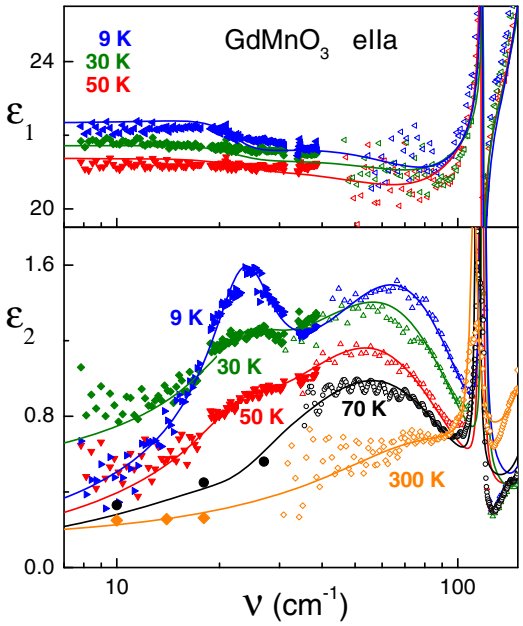

Fig. 2. (Color online) Complex dielectric permittivity of $GdMnO_3$ in the far infrared frequency range. Open symbols – experimental data obtained from transmittance and reflectance spectra, closed symbols – data obtained from the complex transmission coefficient [6,9], solid lines – model based on a sum of Lorentzians.

represents the far-infrared spectra of the dielectric permittivity of $GdMnO_3$ in the frequency range relevant for electromagnons. The results by the infrared transmittance rapidly loose the accuracy below 40 cm^{-1}. Therefore, the data obtained by BWO spectroscopy [6,9] are plotted as closed symbols in this frequency range.

Two strong electromagnons can be well observed in the spectra of the dielectric permittivity in Figure 2 close to 23 cm^{-1} and 75 cm^{-1}. These modes are seen most clearly in the imaginary part of the dielectric permittivity (lower panel). The mode at 23 cm^{-1} has been proven in previous experiments [9] as an electrically active magnon

(electromagnon). On the contrary, solely from the present results the electric character of the high-frequency mode at 75 cm^{-1} cannot be stated unambiguously. Especially the existence of the magnetic excitation channel with $\tilde{h} \| b$ cannot be excluded for our *ab*-oriented sample. However, full analysis of the high-frequency electromagnon carried out for related $RMnO_3$ systems [8,11,26,27] revealed pure electric character of the high-frequency excitation. Therefore, we derive the same conclusion for $GdMnO_3$ as well.

Compared to other multiferroic rare-earth perovskite manganites, $GdMnO_3$ most probably is on the border between multiferroic and non-multiferroic behavior. This fact can be illustrated e.g. by the comparative phase diagram of the rare earth manganites, published recently [28]. As already mentioned in the Introduction section, $GdMnO_3$ does not reveal polar electric order but can be made ferroelectric by applying a magnetic field along the *b*-axis [20,22]. Besides, the incommensurate magnetic state in $GdMnO_3$ is very subtle: the application of a moderate external magnetic field parallel to the *c*-axis easily leads to the commensurate canted antiferromagnetic state and to the suppression of electromagnons [9,25]. After the application of an external magnetic field of only 0.15 T at $T = 15$ K the canted state can be induced and it remains stable even after removing the field [9] (bi-stability). Therefore, it is not surprising that the results obtained on different samples of $GdMnO_3$ may differ from each other as the parameter space of the canted and incommensurate antiferromagnetic states may overlap. This is the reason why much less terahertz absorption in $GdMnO_3$ has been detected in references [8,29] and in the magnetically ordered state. The magnetic phase in these experiments was most probably canted antiferromagnetic in which the magnetoelectric effect is not observed.

In the spectra of the real part of the dielectric permittivity (ε_1, upper panel) only the low-frequency electromagnon can be detected. The high-frequency electromagnon is not seen in the ε_1 spectra because of a small dielectric contribution of this excitation ($\Delta\varepsilon \sim 0.5$) compared to the contributions of the phonons ($\Delta\varepsilon \sim 20$) and to a relatively large noise level between 40 cm^{-1} and 100 cm^{-1}. In order to obtain the parameters of both electromagnons, the dielectric spectra in the far infrared frequency range were fitted using the sum of several Lorentzians. Two low-frequency Lorentzians were responsible for the electromagnons close to 23 cm^{-1} and 75 cm^{-1}, and additional higher frequency modes represented the contribution of the phonons. We took the parameters of the high-frequency phonons in $GdMnO_3$ from reference [25]. In Figure 2 the effect of only the phonon at 120 cm^{-1} is important, and the higher frequency phonons contribute to the low-frequency slope of the dielectric permittivity only.

The dielectric parameters of both electromagnons are shown in Figure 3 as a function of temperature with the resonance positions represented in the left panel. As already mentioned during the discussion of Figure 1, the high-frequency electromagnon can be observed even at $T = 70$ K, i.e. far above the Néel phase transition. The

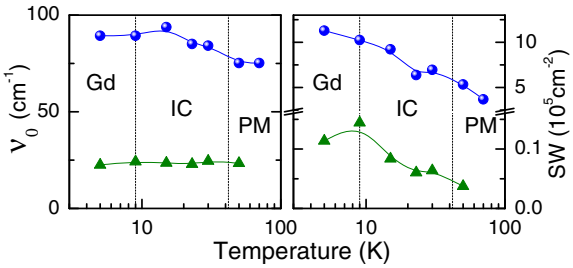

Fig. 3. (Color online) Parameters of the electromagnons in $GdMnO_3$. Left panel – eigenfrequencies, right panel – spectral weight[1] (note change in scale in the vertical axis). Symbols – experimental data, lines are to guide the eye. Thin dashed lines indicate phase boundaries between different magnetic states [20,25]: PM – paramagnetic, IC – incommensurate, Gd – Gadolinium ordering. Note that in present experiments the canted magnetic state is avoided because of zero external magnetic field [9,25].

eigenfrequency of this mode slightly decreases with increasing temperature in the magnetically ordered state. The position of the low-frequency electromagnon remains roughly temperature independent. This mode cannot be detected in the spectra above 50 K. We note that the eigenfrequency especially of the high-frequency electromagnon is slightly higher than the observed maximum in ε_2 (Fig. 2). This is due to to the over-damped character of both electromagnons. Especially the width of the high-frequency electromagnon is quite large $g = 125 \pm 5$ cm^{-1} and, in agreement with the Lorentzian formula, substantially shifts the position of the maximum in ε_2.

Contrary to the temperature independence of the eigenfrequencies, the spectral weight[1] of the electromagnons in $GdMnO_3$ is strongly temperature dependent. On heating the sample into the paramagnetic state, the spectral weight of both electromagnons decreases by about a factor of three. However, the spectral weight of both electromagnons seem to remain finite even in the paramagnetic state, which could probably be related to the antiferromagnetic fluctuations.

At present, the dispute on the nature of the high-frequency electromagnon in orthorhombic multiferroic manganites seems to be settled [11,14]. The frequency of this mode corresponds to the zone-edge magnon, the excitation conditions and the spectral weight are well explained on the basis of Heisenberg-exchange coupled spins. In order to provide an explanation for the low-frequency mode, a magnetic anisotropy [18] and higher harmonics of the spin cycloid [19] within the Heisenberg exchange model have been suggested. The ratio of the frequency positions of both electromagnons $\nu_{0,1}/\nu_{0,2} = 3.7 \pm 0.5$ approximately agrees with the values in the $(Gd{:}Tb)MnO_3$ system [30] and can be accounted for

[1] The spectral weight is a property characterizing the intensity of an excitation and is defined as $SW = \int_0^\infty \mathrm{Re}(\sigma(\omega))d\omega$. In case of a Lorentzian the spectral weight is equal to $SW = \frac{\pi}{2}\varepsilon_0\Delta\varepsilon\omega_0^2$, where ε_0 is the permittivity of vacuum, $\Delta\varepsilon$ and ω_0 are dielectric contribution and eigenfrequency of the Lorentzian, respectively.

by the anisotropy model [18]. On the contrary, the ratio of the spectral weights for $GdMnO_3$ can be estimated as $SW_2/SW_1 = 0.011 \pm 0.002$. Such small values agree with the tendency, observed in the (Gd:Tb)MnO_3 [30], but differ by about an order of magnitude from theoretical estimates [18]. A possible reason for this discrepancy is the absence of the true cycloidal structure in $GdMnO_3$. In contrast to other orthorhombic multiferroic manganites like $TbMnO_3$ or $DyMnO_3$, most probably no cycloidal magnetic structure exists [31] in the ordered state of $GdMnO_3$.

An alternative mechanism for the 23 cm^{-1} mode can be suggested in analogy with the discussion [15,16] of the low-frequency electromagnon in $TbMnO_3$. In this compound the inverse Dzyaloshinskii-Moriya (IDM) mechanism [17,32,33] has been suggested to explain at least a part of the intensity of the low-frequency electromagnon. The basic argument for this suggestion was a coincidence of the excitation frequencies as measured by terahertz spectroscopy [15] and by inelastic neutron scattering [13]. In support of this idea a weak IDM contribution has been recently observed [16] at the field-induced transition in $TbMnO_3$. We recall however that the IDM mechanism explains only few percent of the spectral weight of the low-frequency electromagnon and the Heisenberg exchange mechanism is probably responsible for the remaining intensity.

4 Conclusions

In conclusion, using far infrared transmission spectroscopy, the high-frequency part of the electromagnon spectrum in $GdMnO_3$ has been investigated. The spectral weight of the high-frequency electromagnon is roughly two orders of magnitude higher than that of the low-frequency mode. This ratio is the largest among other orthorhombic manganite multiferroics and cannot be explained within the existing models. The high-frequency electromagnon can be seen in the spectra even deep in the paramagnetic state.

This work was supported by DFG (Pi 372) and by the Transregional Research Center TRR80 (Augsburg/Munich).

References

1. M. Fiebig, J. Phys. D: Appl. Phys **38**, R123 (2005)
2. W. Eerenstein, N.D. Mathur, J.F. Scott, Nature **442**, 759 (2006)
3. S.-W. Cheong, M. Mostovoy, Nat. Mater. **6**, 13 (2007)
4. T. Kimura, T. Goto, H. Shintani, K. Ishizaka, T. Arima, Y. Tokura, Nature **426**, 55 (2003)
5. M. Saito, K. Ishikawa, S. Konno, K. Taniguchi, T. Arima, Nat. Mater. **8**, 634 (2009)
6. A. Pimenov, A.M. Shuvaev, A.A. Mukhin, A. Loidl, J. Phys.: Condens. Matter **20**, 434209 (2008)
7. A.B. Sushkov, M. Mostovoy, R. Valdes Aguilar, S.-W. Cheong, H.D. Drew, J. Phys.: Condens. Matter **20**, 434210 (2008)
8. N. Kida, Y. Takahashi, J.S. Lee, R. Shimano, Y. Yamasaki, Y. Kaneko, S. Miyahara, N. Furukawa, T. Arima, Y. Tokura, J. Opt. Soc. Am. B **26**, A35 (2009)
9. A. Pimenov, A.A. Mukhin, V. Yu. Ivanov, V.D. Travkin, A.M. Balbashov, A. Loidl, Nat. Phys. **2**, 97 (2006)
10. Y. Takahashi, N. Kida, Y. Yamasaki, J. Fujioka, T. Arima, R. Shimano, S. Miyahara, M. Mochizuki, N. Furukawa, Y. Tokura, Phys. Rev. Lett. **101**, 187201 (2008)
11. R. Valdes Aguilar, M. Mostovoy, A.B. Sushkov, C.L. Zhang, Y.J. Choi, S.-W. Cheong, H.D. Drew, Phys. Rev. Lett. **102**, 047203 (2009)
12. R. Kajimoto, H. Mochizuki, H. Yoshizawa, H. Shintani, T. Kimura, Y. Tokura, J. Phys. Soc. Jpn **74**, 2430 (2005)
13. D. Senff, N. Aliouane, D.N. Argyriou, A. Hiess, L.P. Regnault, P. Link, K. Hradil, Y. Sidis, M. Braden, J. Phys.: Condens. Matter **20**, 434212 (2008)
14. S. Miyahara, N. Furukawa, Theory of electric field induced one-magnon resonance in cycloidal spin magnets, `arXiv:0811.4082` (2008)
15. A. Pimenov, A. Shuvaev, A. Loidl, F. Schrettle, A.A. Mukhin, V.D. Travkin, V.Yu. Ivanov, A.M. Balbashov, Phys. Rev. Lett. **102**, 107203 (2009)
16. A.M. Shuvaev, V.D. Travkin, V.Yu. Ivanov, A.A. Mukhin, A. Pimenov, Phys. Rev. Lett. **104**, 097202 (2010)
17. H. Katsura, A.V. Balatsky, N. Nagaosa, Phys. Rev. Lett. **98**, 027203 (2007)
18. M.P.V. Stenberg, R. de Sousa, Phys. Rev. B **80**, 094419 (2009)
19. M. Mochizuki, N. Furukawa, N. Nagaosa, Phys. Rev. Lett. **104**, 177206 (2010)
20. T. Kimura, G. Lawes, T. Goto, Y. Tokura, A.P. Ramirez, Phys. Rev. B **71**, 224425 (2005)
21. J. Hemberger, S. Lobina, H.-A. Krug von Nidda, N. Tristan, V.Yu. Ivanov, A.A. Mukhin, A. M. Balbashov, A. Loidl, Phys. Rev. B **70**, 024414 (2004)
22. J. Baier, D. Meier, K. Berggold, J. Hemberger, A. Balbashov, J.A. Mydosh, T. Lorenz, Phys. Rev. B **73**, 100402 (2006)
23. A.M. Balbashov, S.G. Karabashev, Ya.M. Mukovskiy, S.A. Zverkov, J. Cryst. Growth **167**, 365 (1996)
24. T. Goto, T. Kimura, G. Lawes, A.P. Ramirez, Y. Tokura, Phys. Rev. Lett. **92**, 257201 (2004)
25. A. Pimenov, T. Rudolf, F. Mayr, A. Loidl, A.A. Mukhin, A.M. Balbashov, Phys. Rev. B **74**, 100403 (2006)
26. N. Kida, Y. Ikebe, Y. Takahashi, J.P. He, Y. Kaneko, Y. Yamasaki, R. Shimano, T. Arima, N. Nagaosa, Y. Tokura, Phys. Rev. B **78**, 104414 (2008)
27. Y. Takahashi, Y. Yamasaki, N. Kida, Y. Kaneko, T. Arima, R. Shimano, Y. Tokura, Phys. Rev. B **79**, 214431 (2009)
28. S. Ishiwata, Y. Kaneko, Y. Tokunaga, Y. Taguchi, T. Arima, Y. Tokura, Phys. Rev. B **81**, 100411 (2010)
29. J.S. Lee, N. Kida, S. Miyahara, Y. Takahashi, Y. Yamasaki, R. Shimano, N. Furukawa, Y. Tokura, Phys. Rev. B **79**, (R)180403 (2009)
30. J.S. Lee, N. Kida, Y. Yamasaki, R. Shimano, Y. Tokura, Phys. Rev. B **80**, 134409 (2009)
31. T. Kimura, S. Ishihara, H. Shintani, T. Arima, K.T. Takahashi, K. Ishizaka, Y. Tokura, Phys. Rev. B **68**, 060403 (2003)
32. H. Katsura, N. Nagaosa, A.V. Balatsky, Phys. Rev. Lett. **95**, 057205 (2005)
33. I.A. Sergienko, E. Dagotto, Phys. Rev. B **73**, 094434 (2006)